Atmospheric Research 285 (2023) 106645

Contents lists available at ScienceDirect

Atmospheric Research

journal homepage: www.elsevier.com/locate/atmosres

On coarse patterns in the atmospheric concentration of ice nucleating particles

Franz Conen [a,*], Mikhail V. Yakutin [b], Alexander N. Puchnin [c], Karl Espen Yttri [d]

[a] Department of Environmental Sciences, University of Basel, Basel, Switzerland
[b] Institute of Soil Science and Agrochemistry, Siberian Branch of the Russian Academy of Sciences, 630090 Novosibirsk, Russia
[c] Yakutian State Agricultural Academy, Yakutsk, Republic of Sakha (Yakutia), Russia
[d] NILU – Norwegian Institute for Air Research, Kjeller, Norway

ARTICLE INFO

Keywords:
Ice nucleating particles
Observations
Large-scale pattern

ABSTRACT

The atmospheric concentration of ice nucleating particles active at around −10 °C (INP_{-10}) is very low. Nevertheless, these particles play a role in the development of cloud systems, so their spatial and temporal patterns merit attention. We collated available datasets on INP_{-10} to identify such patterns. Among the five low altitude observatories in northern Eurasia, median values throughout May to October were lowest in Scandinavia (4 and 6 m^{-3}), somewhat higher in central Europe (11 m^{-3}), substantially higher in the West Siberian Plain (69 m^{-3}) and highest in the Central Yakutian Lowland (204 m^{-3}), suggesting that the abundance of INP_{-10} in northern Eurasia may increase with continentality and from West to East. The range of values at the same observatories was narrower throughout November to April (2 to 27 m^{-3}). On average, by an order of magnitude smaller values were reported for the four Arctic observatories. Consequently, increasing poleward transport of air masses from the midlatitudes likely raises the concentration of INP_{-10} in the Arctic, particularly when air masses had surface contact in eastern parts of northern Eurasia.

1. Introduction

The transient existence of clouds is subject to meteorological and microphysical conditions (Findeisen, 1938). Ice nucleating particles (INPs) modify microphysical conditions in cloud droplets by lowering the energy barrier to be overcome in the transition from supercooled liquid to ice (Kanji et al., 2017). Certain bacteria, fungal spores and macromolecules aerosolised from vegetation and plant litter act as INPs at a few degrees below 0 °C (Sands et al., 1982; Lindemann et al., 1982; Vasebi et al., 2019). Yet, their concentration in clouds is very low (Joly et al., 2014). To quantify these INPs in the atmosphere a sufficient number of them needs to be collected, typically from several cubic metres of air, and analysed off-line in a drop freeze assay. Demands on time and manual labour limit the data made available through such observations. When temperature drops below about −15 °C, increasingly other kinds of aerosol particles cause freezing of cloud droplets (Murray et al., 2012; Kanji et al., 2017; Huang et al., 2021). At −30 °C the vast majority of INPs above central Europe is contributed by desert dust (Brunner et al., 2021), in which feldspar may be the most active ingredient (Atkinson et al., 2013). The greater abundance of INPs active at −30 °C allows reliable quantification in several litres air through real-time, automated measurement (Brunner and Kanji, 2021).

When there is enough moisture available for the activation of INPs, the number concentration of activated INPs increases with decreasing temperature of an air mass. Hawker et al. (2021) have demonstrated how the slope of this relation determines the development of a convective cloud system. A shallow slope, which compared to a steep slope has a larger number of INPs activated above −17 °C and a smaller number below −17 °C, led their regional model to predict ice formation at lower altitudes and resultingly reduced anvil development, with an overall reduced outgoing radiation from cloudy regions. Also, shallow cumulus clouds can be affected by INPs active at little supercooling as shown by modelling (Mason, 1996) and observation (Crosier et al., 2011; Crawford et al., 2012). Such clouds form precipitation when initial ice formation by INPs is amplified through secondary ice production (Field et al., 2017; Phillips et al., 2017; Sullivan et al., 2018). Increasing concentration of INP may promote precipitation and thereby reduce cloud lifetime, resulting in a positive climate feedback (Murray et al., 2021). Low-level mixed-phase clouds in the Arctic are a further example, where the concentration of INPs active at little supercooling

* Corresponding author.
E-mail address: franz.conen@unibas.ch (F. Conen).

https://doi.org/10.1016/j.atmosres.2023.106645
Received 16 September 2022; Received in revised form 30 January 2023; Accepted 2 February 2023
Available online 9 February 2023
0169-8095/© 2023 The Author(s). Published by Elsevier B.V. This is an open access article under the CC BY license (http://creativecommons.org/licenses/by/4.0/).

probably makes a difference to cloud lifetime and radiation properties (Morrison et al., 2012; Pasquier et al., 2022).

While the number concentration of INPs active below −15 °C can be estimated from the more easily measured number concentration of aerosol particles >0.5 μm (DeMott et al., 2015) combined with the history of an air mass (Mignani et al., 2021), the same does not necessarily hold true for INPs active at around −10 °C (Conen et al., 2015). Although, the number concentration of INPs active at −16 °C tends to increase with increasing PM_{10} mass concentration, INPs active at −12 or −8 °C are completely unrelated to this parameter (Welti et al., 2018a, 2018b). The lack of correlation probably results from INP_{-10} having different sources from the majority of similar-sized aerosol particles and the minute share of INP_{-10} among them. Aerosol properties more specifically related to biological INPs, such as particle fluorescence, are available only for a very limited number of short studies in combination with measurements of INPs active well below −10 °C (Huffman et al., 2013; Prenni et al., 2013).

Perhaps, the distribution of vegetation and climatic zones is a more applicable predictor of INP_{-10}. Schnell and Vali (1973) discovered that the number concentration of INP_{-10} produced by decaying leaves increases from the tropics to temperate rainy environments and is highest in zones with a cold winter. In addition, a corresponding trend in the atmospheric concentration of INP active at −15 °C was identified by Schnell and Vali (1976) for measurements available at that time and from which they had excluded those made under snowbound conditions. Frequent freeze-thaw cycles excert selective pressure on diverse populations of microorganisms to the advantage of those that are ice-nucleation active (Wilson et al., 2012). In addition, microorganisms can substantially increase the production of ice-nucleation active molecules when growing at cold temperature (Yang et al., 2022). Therefore, colder environments may harbour a larger fraction of ice-nucleation active microorganisms.

Geographical boundaries of climatic zones are shifting (Beck et al., 2018). The same probably applies to vegetation as the source of INP_{-10}. A higher plant productivity and expanding forest cover is already observed in the far North of Russia (Schaphoff et al., 2016). However, aerosolisation of INP_{-10} from standing or decaying vegetation is also modulated by other drivers that are subject to climate change. A major driver of INP aerosolisation is rainfall (Bigg and Miles, 1964; Huffman et al., 2013; Mignani et al., 2021; Gong et al., 2022), but not snowfall (Hara et al., 2016; Conen et al., 2017a); a major suppressor is snow cover (Conen et al., 2017a; Creamean et al., 2018). Large-scale continuous observations are necessary to reveal likely changes in the atmospheric concentration of INP_{-10} concurrent with shifts in climate zones and changing weather pattern. Such observations should be designed to address specific needs of climate models, which are indispensable to unravel the sign and magnitude of complex INP-cloud-climate interactions (Burrows et al., 2009). Here, we summarise available data on INP_{-10} with the objective to identify large scale and coarse temporal patterns that may inform the planning of future observations.

Fig. 1. Location of observatories at which INP concentrations were measured that are summarised in this study. The dotted line indicates the Arctic Circle.

2. Material and methods

We collated datasets from 11 observatories (Fig. 1) in the Northern Hemisphere reporting on INPs active between −8 and − 12 °C for both the colder and the warmer half of the year. They include datasets available under a Creative Commons License (CC BY 4.0 or CC BY 3.0) plus own datasets acquired during earlier studies. All field studies during which these data were acquired, except the one in Yakutsk, are described and discussed in the publications referred to in Table 1.

At nine observatories procedures were very similar. Whereever vegetation was present, air was sampled from above the canopy, including trees. Particulate matter <10 μm (PM_{10}) was collected on Quartz fibre filters and millimetre-size pieces of these filters were analysed for INPs in immersion freezing assays. Size cut-off is not mentioned in the studies reporting data for Ny-Alesund and Alert (Wex et al., 2019a), but data at Ny-Alesund was definitively derived from PM_{10} samples as reported later by Rinaldi et al. (2021). In contrast, sampling at Alert was probably different. Rodriguez et al. (2020) report to have sampled total suspended particles at the same observatory in Alert as Wex et al. (2019a), with an instrument that shares characteristics (custom-built, flow rate, filter-size, location) with the instrument mentioned in Wex et al. (2019a). Therefore, the concentration of INP_{-10} could be somewhat larger at Alert than might have been, if PM_{10} was sampled. Also, the data from Hyytiälä (Schneider et al., 2021) is potenitally higher than it might have been, if the same procedures had been followed as at the nine observatories mentioned before. The use of membrane filters at Hyytiälä is unlikely to have made a difference. Yet, sampling below the canopy may have resulted in a higher concentration of INP_{-10} as compared to sampling above the canopy (Seifried et al., 2021).

In Yakutsk, aerosol particles were collected on Quartz fibre filters (Pallflex® Tissuequartz, effective diameter 38 mm, Pall Corporation, Port Washington, NY, USA) using a low-volume sampler (PQ100, BGI, Mesa Labs Inc., Butler, NJ, USA) with a PM_{10} inlet operating at a flow rate of 16.7 L min^{-1}. The sampler was situated with its inlet about 5 m above ground level on the roof of a house in the southern outskirts of the city of Yakutsk. Eventual air pollution is unlikely to affect INP concentration (Chen et al., 2018). Twenty aerosol particle samples with an average sampling time of 10 h were collected throughout the year 2018 (more details in Supplement A) and analysed for INPs following the method described in Conen et al. (2012). Briefly, 72 filter pieces with 1 mm diameter were cut from each filter sample and each piece was immersed in high-purity water (100 μL) in an Eppendorf safe-lock tube (0.5 mL) and exposed to decreasing temperature (0.33C min^{-1}) in a cold bath. The number of frozen tubes was counted by eye after each 1 °C step. Cumulative number concentration of INPs were calculated as proposed by Vali (1971). Blank (background) values were determined for five filters by analysing filter pieces with 1 mm diameter from their 5 mm wide fringe, which had been clamped into the filter holder during sampling and was not exposed to the airstream. We subtracted the median of blank values from the median of sample values.

The coarse pattern we intended to identify concern differences in the median INP concentration between observatories. Hereby, we distinguished between the warmer (01. May to 31. October) and the colder (01. November to 30. April) part of the year. A median does justice to the log-normal distribution of INPs (Welti et al., 2018a), where it is equal to the geometric mean ($\bar{x}^*$). Further, the median can accomodate values below and above detection limit as long as each category constitutes <50% of the total number of values. The log-normal distribution of INPs is best characterised by the multiplicative standard deviation (s^*), estimated robustly as: [upper quartile/lower quartile]$^{0.741}$ (Limpert et al., 2001). Approximately 68% of all values are between $\bar{x}^*$ times s^* and $\bar{x}^*$ divided by s^*, and around 95% of all values are between $\bar{x}^*$ times $(s^*)^2$ and $\bar{x}^*$ divided by $(s^*)^2$ (Limpert et al., 2001).

3. Results and discussion

There is a large variation between observatories and seasons in terms of the number of samples available (Table 1). However, the multiplicative standard deviation (s^*) of the median did not systematically change with sample number. Values of s^* for INP_{-10} ranged from 2.2 (Utqiagvik, May–October, $n = 20$) to 9.3 (Chaumont, November–April, $n = 36$). In 10 of 22 cases s^* had a value between 2.5 and 3.6, and in 5 cases it could not be estimated because the lower or upper quartile of the samples had values outside the detection limits (May–October: Villum and Alert; November–April: Villum, Ny-Alesund, and Hyytiälä) (Fig. 2).

The median concentration of INP_{-10} differed substantially between observatories and at half of the observatories also between the warmer and the colder half of the year. Earlier, the work of Schrod et al. (2020) had revealed *"fairly similar"* average concentration of INPs at four observatories, including two in the tropics, one in the midlatitudes, and one in the Arctic. Annual cycles were not observed in any of these two-year time series (Schrod et al., 2020). These different findings could be because Schrod et al. (2020) investigated INPs across a lower temperature range (−20 to −30 °C) where potential sources might be more evenly distributed. Also, aerosolisation, activation and deposition might vary less between seasons than seems to be the case with INP_{-10}.

3.1. May to October

Most measurements made in northern Eurasia during the warmer half of the year had values of $INP_{-10} \geq 10$ m^{-3} (Table 1), except in Scandinavia (Birkenes, Hyytiälä), where such concentrations occurred only in around 30% of the samples. Median values at the five observatories in northern Eurasia ranged from 4 to 204 INP_{-10} m^{-3}, with higher values at more continental sites. At three observatories within the same climatic zone (Novosibirsk, Chaumont, Birkenes) median values increased by an order of magnitude from the coastal (Birkenes) to the extremely continental site (Novosibirsk), with the central European site in between. Highest concentrations were found at the easternmost observatory, in the Central Yakutian Lowland (Yakutsk), a permafrost region experiencing very cold winters, but nevertheless vegetated with larch, birch and meadows. This apparent West-East gradient in INP_{-10} across northern Eurasia (Fig. 2, left-hand panel) resembles that of bacteria in near-surface air (Burrows et al., 2009), where values also increase from western Europe through Siberia to the Central Yakutian Lowland. In contrast, modeled surface concentration of INPs active at −15 °C associated with K-feldspar (Vergara-Temprado et al., 2017) shows a two orders of magnitude lower value in the Central Yakutian Lowland, as compared with central Europe. Feldspar and other mineral particles are the predominant form of atmospheric INPs active in the colder half of the heterogeneous freezing range (Suski et al., 2018; Huang et al., 2021; Brunner et al., 2021). Because of the opposite West-East trends in INPs active at warmer and at colder temperatures the full INP spectrum (−3 to −38 °C) is probably steep in the western and shallow in the eastern part of northern Eurasia. Yet, little of that is visible in the narrow temperature window from −8 to −12 °C (Table 1). Exponential regressions fitted to INP as a function of temperature indicate an increase in INPs by a factor of only 1.5 and 1.6 per 1 degree of cooling ($°C^{-1}$) at Chaumont and Birkenes and a larger factor at Yakutsk (1.9 $°C^{-1}$) and Novosibirsk (1.9 $°C^{-1}$), but the factor at Hyytiälä was similarly large (2.0 $°C^{-1}$). Still, these trends can not be extrapolated to much colder temperatures because an INP spectrum does not necessarily follow a simple exponential function from −3 to 38 °C (Petters and Wright, 2015; Creamean et al., 2018; Testa et al., 2021).

Overall, median concentration of INP_{-10} between May and October was up to two orders of magnitude higher in northern Eurasia as compared to the Arctic, where values of $INP_{-10} \geq 10$ m^{-3} occurred in only 3 of 47 measurements (Table 1). Nevertheless, the smallest median observed in northern Eurasia (3.9 m^{-3}), at a coastal site (Birkenes), was very close to the largest median found in the Arctic region, also at a

Table 1
Summarised observations of INPs active between −8 and −12 °C. Köppen-Geiger climate class is taken from a map with 0.0083° resolution produced by Beck et al. (2018).

Site description						Observations of ice nucleating particles (INPs)								Reference of study
Observatory	Year	Latitude	Longitude	Altitude	Köppen-Geiger climate class	Months	n	Median concentration (m^{-3})					Fraction of observations with INPs at −10 °C		[reference of dataset]
				(m a.s.l.)				−8 °C	−9 °C	−10 °C	−11 °C	−12 °C	≥ 1 m^{-3}	≥10 m^{-3}	
Yakutsk	2018	61.97° N	129.67° E	100	Cold, no dry season, very cold winter	May - Oct	13	37.1	109.1	204.3	324.6	541.2	1.00	1.00	This study
						Nov - Apr	7	7.6	27.9	27.1	63.2	87.2	0.86	0.86	[This study, Supplement A]
						ratio		*4.9*	*3.9*	*7.5*	*5.1*	*6.2*			
Novosibirsk	2016–2017	54.85° N	83.10° E	150	Cold, no dry season, warm summer	May - Oct	30	15.1	38.9	68.6	115.8	n.a.	1.00	0.97	Conen et al., 2017b
						Nov - Apr	26	1.6	4.5	7.5	13.0	18.6	1.00	0.34	[This study, Supplement B]
						ratio		*9.4*	*8.7*	*9.1*	*8.9*	n.a.			
Chaumont	2012–2013	47.05° N	06.98° E	1136	Cold, no dry season, warm summer	May - Oct	36	5.9	9.0	11.2	16.0	28.7	1.00	0.58	Conen et al., 2015
						Nov - Apr	36	1.5	3.0	8.5	12.8	19.8	0.72	0.44	[This study, Supplement C]
						ratio		*3.9*	*3.0*	*1.3*	*1.3*	*1.4*			
Hyytiälä	2018–2019	61.85° N	24.29° E	181	Cold, no dry season, cold summer	May - Oct	99	1.3	3.2	5.7	11.7	21.9	0.96	0.28	Schneider et al., 2021
						Nov - Apr	117	n.a.	0.8	2.2	5.1	7.8	0.66	0.06	[Schneider et al., 2020]
						ratio		n.a.	*3.9*	*2.6*	*2.3*	*2.8*			
Birkenes	2013–2014	58.38° N	08.25° E	219	Cold, no dry season, warm summer	May - Oct	31	1.5	3.0	3.9	6.5	10.2	1.00	0.29	Conen et al., 2017a
						Nov - Apr	35	2.6	4.3	6.9	8.8	12.0	0.94	0.43	[This study, Supplement D]
						ratio		*0.6*	*0.7*	*0.6*	*0.7*	*0.9*			
Ny-Ålesund	2012	78.91° N	11.88° E	40*	Polar, tundra	May - Oct	10	0.46	1.11	2.27	3.76	5.61	0.80	0.00	Wex et al., 2019a
						Nov - Apr	3	0.12	0.12	0.23	0.36	0.60	0.00	0.00	[Wex et al., 2019b]
						ratio		*4.0*	*9.5*	*9.7*	*10.6*	*9.3*			
Villum	2013, 2015	81.60° N	16.67° W	24	Polar, tundra	May - Oct	4	0.34	2.59	n.a.	n.a.	n.a.	0.75	0.50	Wex et al., 2019a
						Nov - Apr	7	0.07	0.27	0.64	1.04	1.79	0.29	0.14	[Wex et al., 2019c]
						ratio		*5.2*	*9.6*	n.a.	n.a.	n.a.			
Alert	2015–2016	82.50° N	62.37° W	200	Polar, tundra	May - Oct	13	0.77	1.85	3.47	6.69	8.09	0.62	0.00	Wex et al., 2019a
						Nov - Apr	25	0.37	0.79	1.52	2.28	2.78	0.56	0.04	[Wex et al., 2019d]
						ratio		*2.1*	*2.4*	*2.3*	*2.9*	*2.9*			
Utqiagvik	2012–2013	71.30° N	156.77° W	60	Polar, tundra	May - Oct	20	0.36	0.83	1.63	2.61	3.64	0.70	0.05	Wex et al., 2019a
						Nov - Apr	21	0.02	0.05	0.15	0.41	0.32	0.19	0.00	[Wex et al., 2019e]
						ratio		*18.1*	*16.3*	*10.6*	*6.4*	*11.4*			
Jungfraujoch	2012–2013	46.55° N	07.98° E	3580	Polar, tundra	May - Oct	47	1.14	2.50	3.95	5.43	7.73	0.85	0.15	Conen et al., 2015
						Nov - Apr	36	0.03	0.19	0.47	0.65	0.91	0.22	0.03	[This study, Supplement E]
						ratio		*38.0*	*13.2*	*8.4*	*8.4*	*8.5*			
Cape Verde	2008–2013	16.85° N	24.87° W	30	Arid, desert, hot	May - Oct	210	0.27	0.55	0.96	1.57	2.44	0.50	0.05	Welti et al., 2018a
						Nov - Apr	284	0.27	0.64	1.36	2.20	3.38	0.58	0.02	[Welti et al., 2018b]
						ratio		*1.0*	*0.9*	*0.7*	*0.7*	*0.7*			

* From Rinaldi et al. (2021).

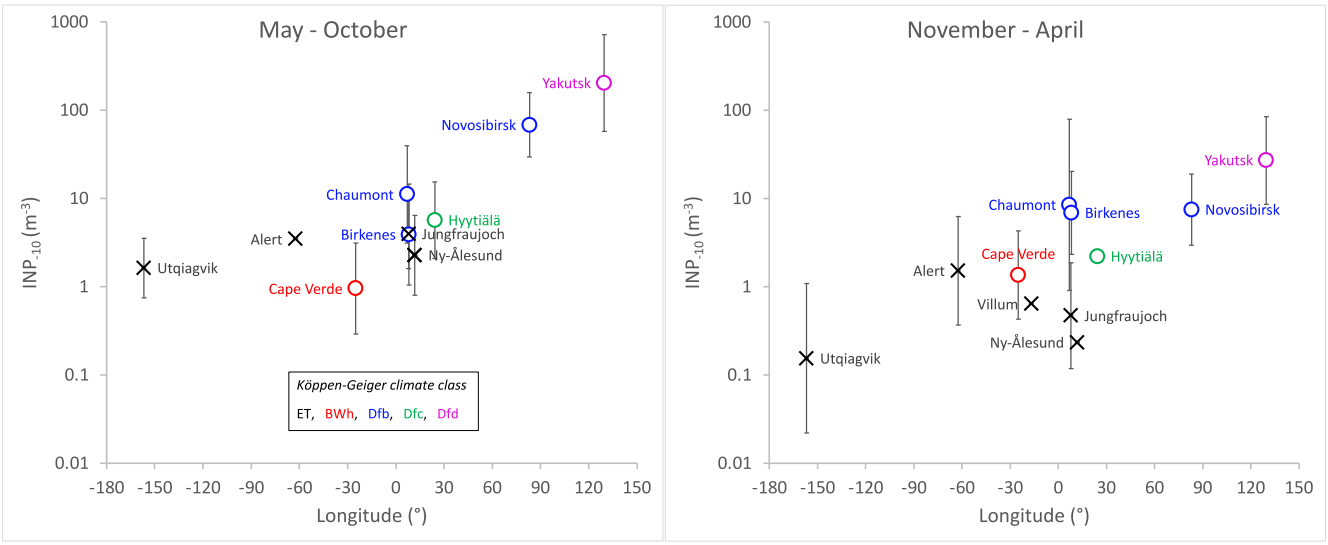

Fig. 2. Median atmospheric INP_{-10} concentration at 11 observatories alligned by longitude. Observatories are colour-coded according to the Köppen-Geiger climate class that corresponds with their location (Beck et al., 2018). Error bars (multiplicative standard deviation) indicate the range including approximately 68% of the observed values. For the observatory Villum available measurements did not provide for determining a median value for May to October, and for some observatories it was not possible to estimate the multiplicative standard deviation in both seasons because more than a quarter of samples were either above or below detection limit.

coastal site (Alert, 3.5 m^{-3}). Values of INP_{-10} differed little between Arctic sites and were like those at the high altitude observatory Jungfraujoch (3580 m a.s.l.) in central Europe and at the Cape Verde Atmospheric Observatory (30 m a.s.l.) in the subtropical marine environment of Cabo Verde.

3.2. November to April

During the colder half of the year, four of five low-altitude observatories in northern Eurasia reported values ≥10 INP_{-10} m^{-3} for more than one-third of all measurements and all observatories had at least two-thirds of all measured values ≥1 INP_{-10} m^{-3}. Difference within northern Eurasia was within one order of magnitude in the colder half of the year, except for the high-altitude observatory Jungfraujoch with values similar to those at Arctic observatories. At the three observatories within the same climatic zone (Novosibirsk, Chaumont, Birkenes), median values were almost identical (6.9 to 8.5 INP_{-10} m^{-3}) (Fig. 2b, right-hand panel). Overall, median values in northern Eurasia still tended to be one order of magnitude larger than those observed in the Arctic during the same time of the year, where most measured values were < 1 INP_{-10} m^{-3}.

3.3. Seasonality

Substantially smaller (> factor of 7) median values of INP_{-10} during the colder half as compared to the warmer half of the year were found at the two most continental observatories (Yakutsk, Novosibirsk), two (perhaps three) Arctic observatories (Ny-Ålesund, Utqiagvik, [Villum]) and at the high altitude observatory (Jungfraujoch) (Table 1). Warming probably results in an increased INP_{-10} median concentration at these sites during the colder half of the year, partly because INP emissions are strengthened when bare land is exposed for longer due to reduced snow cover (Irish et al., 2019), and partly because the potential sink of INP_{-10} is weakened. Under warmer conditions INP_{-10} are less likely to be activated and deposited with the ice crystals they have assisted to form (Stopelli et al., 2015), as indicated in an earlier study at the high altitude observatory Jungfraujoch (Conen et al., 2022). Minor seasonality was observed at the marine (Cape Verde) and at the less continental observatories (Chaumont, Hyytiälä). There, warming alone may not affect INP_{-10} concentration as much as it might do at the other observatories. The same probably applies to the coastal observatory (Birkenes), where the median value of INP_{-10} was slightly larger in the colder as compared to the warmer part of the year. Rainfall is the main driver of INPs at Birkenes and was more abundant during the colder part of the measurement period (Conen et al., 2017). Interestingly, the same observation, a rain-driven abundance of INP_{-10} and a higher median value during the colder part of the year, was made by Gong et al. (2022) at Punta Arenas, a coastal site in the very South of Chile.

3.4. Synthesis and implications

Coarse patterns in the atmospheric concentration of INP_{-10} are apparent in space and time. During the warmer half of the year INP_{-10} likely start to accumulate in air masses once they have passed the coast and move into northern Eurasia, possibly tilting INP spectra to increasingly shallower slopes from West to East. Already a one-day passage above land can markedly increase atmospheric concentration of biological INPs (Conen et al., 2016). Further, increasingly colder climates from West to East (Beck et al., 2018) most likely provide for stronger sources of INP_{-10} in eastern as compared to western parts of northern Eurasia (Schnell and Vali, 1973, 1976; Yang et al., 2022). Although INP_{-10} are efficiently removed from clouds with precipitation (Stopelli et al., 2015), they are at the same time aerosolised when rainfall impacts on land (Bigg and Miles, 1964; Huffman et al., 2013; Mignani et al., 2021; Gong et al., 2022). The overall effect can be a net increase in the atmospheric concentration of biological INPs, while simultaneously that of mineral INPs active at cold temperatures is decreased (Testa et al., 2021). The net accumulation of INP_{-10} appears to be limited during the colder half of the year, when precipitation is more likely to reach land surface in form of snowfall and large areas in the interior of the continent are snow-covered. Nevertheless, the concentration of INP_{-10} remains much higher in the eastern part of northern Eurasia as compared to the Arctic.

Storm tracks entering the Arctic from the midlatitudes increase in number and intensity because of climate change (Zhang et al., 2004; Bintanja et al., 2020). Midlatitude air masses advected by such storms have the potential to raise the concentration of INP_{-10} at least temporarily. Based on the patterns observed in this study, we expect storms to have a large impact on Arctic INP_{-10} concentration when air masses have been in contact with eastern parts of northern Eurasia. A smaller

impact is expected when air masses have entered from western or northern parts of Europe, particularly so during the warmer half of the year, when the relative difference in INP_{-10} concentration between Europe and the Arctic seems to be comparatively small. However, as isotherms shift upwards also at the height of mixed-phase Arctic clouds (typically 0.5 to 2 km; Morrison et al., 2012), the likelihood declines that INP_{-10} are activated under ambient conditions. Changes in storms and isotherms combined, the frequency of primary ice formation at around −10 °C may change little in Arctic clouds. In contrast, where the concentration of INP_{-10} is already high and not expected to change, such as in the Central Yakutian Lowland, the sole upward shift of isotherms may reduce cloud ice formation and result in a negative cloud feedback (Murray et al., 2021).

Funding

The study was financially supported and carried out according to the state assignment of Institute of Soil Science and Agrochemistry of the Siberian Branch of the Russian Academy of Sciences.

Declaration of Competing Interest

The authors declare that they have no known competing financial interests or personal relationships that could have appeared to influence the work reported in this paper.

Data availability

All INP data used in this study is either available from data repositories or as supplementary material to this study.

Acknowledgements

We thank André Welti, Heike Wex, Julia Schneider, and their co-workers for making valuable datasets freely available under Creative Commons licenses. We express our gratitude to Lauren Zweifel for producing Fig. 1. The manuscript has substantially benefitted from helpful reviewer comments and suggestions.

Appendix A. Supplementary data

Supplementary data to this article can be found online at https://doi.org/10.1016/j.atmosres.2023.106645.

References

Atkinson, J., Murray, B., Woodhouse, M., Whale, T.F., Baustian, K.J., Carslaw, K.S., Dobbie, S., O'Sullivan, D., Malkin, T.L., 2013. The importance of feldspar for ice nucleation by mineral dust in mixed-phase clouds. Nature 498, 355–358. https://doi.org/10.1038/nature12278.

Beck, H., Zimmermann, N., McVicar, T., Vergopolan, N., Berg, A., Wood, E.F., 2018. Present and future Köppen-Geiger climate classification maps at 1-km resolution. Sci. Data 5, 180214. https://doi.org/10.1038/sdata.2018.214.

Bigg, E.K., Miles, G.T., 1964. The results of largescale measurements of natural ice nuclei. J. Atmos. Sci. 21, 396–403. https://doi.org/10.1175/1520-0469(1964)021<0396:TROLMO>2.0.CO;2.

Bintanja, R., van der Wiel, K., van der Linden, E.C., Reusen, J., Bogerd, L., Krikken, F., Selten, F.M., 2020. Strong future increases in Arctic precipitation variability linked to poleward moisture transport. Sci. Adv. 6, eaax6869. https://doi.org/10.1126/sciadv.aax6869.

Brunner, C., Kanji, Z.A., 2021. Continuous online monitoring of ice-nucleating particles: development of the automated Horizontal Ice Nucleation Chamber (HINC-Auto). Atmos. Meas. Tech. 14, 269–293. https://doi.org/10.5194/amt-14-269-2021.

Brunner, C., Brem, B.T., Martine Coen, M., Conen, F., Hervo, M., Henne, S., Steinbacher, M., Gysel-Beer, M., Kanji, Z.A., 2021. The contribution of Saharan dust to the ice nucleating particle concentrations at the High Altitude Station Jungfraujoch, Switzerland. Atmos. Chem. Phys. 21, 18029–18053. https://doi.org/10.5194/acp-21-18029-2021.

Burrows, S.M., Butler, T., Jöckel, P., Tost, H., Kerkweg, A., Pöschl, U., Lawrence, M.G., 2009. Bacteria in the global atmosphere – part 2: Modeling of emissions and transport between different ecosystems. Atmos. Chem. Phys. 9, 9281–9297. https://doi.org/10.5194/acp-9-9281-2009.

Chen, J., Wu, Z., Augustin-Bauditz, S., Grawe, S., Hartmann, M., Pei, X., Liu, Z., Ji, D., Wex, H., 2018. Ice-nucleating particle concentrations unaffected by urban air pollution in Beijing. China. Atmos. Chem. Phys. 18, 3523–3539. https://doi.org/10.5194/acp-18-3523-2018.

Conen, F., Henne, S., Morris, C.E., Alewell, C., 2012. Atmospheric ice nucleators active ≥−12°C can be quantified on PM_{10} filters. Atmos. Meas. Tech. 5, 321–327. https://doi.org/10.5194/amt-5-321-2012.

Conen, F., Rodriguez, S., Hüglin, C., Henne, S., Herrmann, E., Bukowiecki, N., Alewell, C., 2015. Atmospheric ice nuclei at the high-altitude observatory Jungfraujoch, Switzerland. Tellus B 67 (25), 014. https://doi.org/10.3402/tellusb.v67.25014.

Conen, F., Stopelli, E., Zimmermann, L., 2016. Clues that decaying leaves enrich Arctic air with ice nucleating particles. Atmos. Environ. 129, 91–94. https://doi.org/10.1016/j.atmosenv.2016.01.027.

Conen, F., Eckhardt, S., Gundersen, H., Stohl, A., Yttri, K.E., 2017a. Rainfall drives atmospheric ice-nucleating particles in the coastal climate of southern Norway. Atmos. Chem. Phys. 17 https://doi.org/10.5194/acp-17-11065-2017, 11 065–11 073.

Conen, F., Yakutin, M.V., Yttri, K.E., Hüglin, C., 2017b. Ice nucleating particle concentrations increase when leaves fall in autumn. Atmosphere 8, 202. https://doi.org/10.3390/atmos8100202.

Conen, F., Einbock, A., Mignani, C., Hüglin, C., 2022. Measurement report: Ice nucleating particles active ≥−15°C in free tropospheric air over western Europe. Atmos. Chem. Phys. 22, 3433–3444. https://doi.org/10.5194/acp-22-3433-2022.

Crawford, I., Bower, K.N., Choularton, T.W., Dearden, C., Crosier, J., Westbrook, C., Capes, G., Coe, H., Connolly, P.J., Dorsey, J.R., Gallagher, M.W., Williams, P., Trembath, J., Cui, Z., Blyth, A., 2012. Ice formation and development in aged, wintertime cumulus over the UK: observations and modelling. Atmos. Chem. Phys. 12, 4963–4985. https://doi.org/10.5194/acp-12-4963-2012.

Creamean, J.M., Kirpes, R.M., Pratt, K.A., Spada, N.J., Maahn, M., de Boer, G., Schnell, R. C., China, S., 2018. Marine and terrestrial influences on ice nucleating particles during continuous springtime measurements in an Arctic oilfield location. Atmos. Chem. Phys. 18, 18023–18042. https://doi.org/10.5194/acp-18-18023-2018.

Crosier, J., Bower, K.N., Choularton, T.W., Westbrook, C.D., Connolly, P.J., Cui, Z.Q., Crawford, I.P., Capes, G.L., Coe, H., Dorsey, J.R., Williams, P.I., Illingworth, A.J., Gallagher, M.W., Blyth, A.M., 2011. Observations of ice multiplication in a weakly convective cell embedded in supercooled mid-level stratus. Atmos. Chem. Phys. 11, 257–273. https://doi.org/10.5194/acp-11-257-2011.

DeMott, P.J., Prenni, A.J., McMeeking, G.R., Sullivan, R.C., Petters, M.D., Tobo, Y., Niemand, M., Möhler, O., Snider, J.R., Wang, Z., Kreidenweis, S.M., 2015. Integrating laboratory and field data to quantify the immersion freezing ice nucleation activity of mineral dust particles. Atmos. Chem. Phys. 15, 393–409. https://doi.org/10.5194/acp-15-393-2015.

Field, R.P., Lawson, R.P., Brown, P.R.A., Lloyd, G., Westbrook, C., Moisseev, D., Miltenberger, A., Nenes, A., Blyth, A., Choularton, D., Connolly, P., Buehl, J., Crosier, J., Cui, Z., Dearden, C., DeMott, P., Flossmann, A., Heymsfield, A., Huang, Y., Kalesse, H., Kanji, Z.A., Korolev, A., Kirchgaessner, A., Lasher-Trapp, S., Leisner, T., McFarquhar, G., Phillips, V., Stith, J., Sullivan, S., 2017. Secondary ice production: current state of the science and recommendations for the future. Meteorol. Monogr. 58, 7.1-7.20. https://doi.org/10.1175/AMSMONOGRAPHS-D-16-0014.1.

Findeisen, W., 1938. Die kolloidmeteorologischen Vorgänge bei der Niederschlagsbildung (Colloidal meteorological processes in the formation of precipitation). Meteorol. Z. 55, 121-133 (translated and edited by Volken, E., Giesche, A.M., Brönnimann, S., 2015. Meteorol. Z), 24. https://doi.org/10.1127/metz/2015/0675.

Gong, X., Radenz, M., Wex, H., Seifert, P., Ataei, F., Henning, S., Baars, H., Barja, B., Ansmann, A., Stratmann, F., 2022. Significant continental source of ice-nucleating particles at the tip of Chile's southernmost Patagonia region. Atmos. Chem. Phys. 22, 10505–10525. https://doi.org/10.5194/acp-22-10505-2022.

Hara, K., Maki, T., Kobayashi, F., Kakikawa, M., Wada, M., Matsuki, A., 2016. Variations of ice nuclei concentration induced by rain and snowfall within a local forested site in Japan. Atmos. Environ. 127, 1–5. https://doi.org/10.1016/j.atmosenv.2015.12.009.

Hawker, R.E., Miltenberger, A.K., Wilkinson, J.M., Hill, A.A., Shipway, B.J., Cui, Z., Cotton, R.J., Carslaw, K.S., Field, P.R., Murray, B.J., 2021. The temperature dependence of ice-nucleating particle concentrations affects the radiative properties of tropical convective cloud systems. Atmos. Chem. Phys. 21, 5439–5461. https://doi.org/10.5194/acp-21-5439-2021.

Huang, S., Hu, W., Chen, J., Wu, Z., Zhang, D., Fu, P., 2021. Overview of biological ice nucleating particles in the atmosphere. Environ. Int. 146, 106197 https://doi.org/10.1016/j.envint.2020.106197.

Huffman, J.A., Prenni, A.J., DeMott, P.J., Pöhlker, C., Mason, R.H., Robinson, N.H., Fröhlich-Nowoisky, J., Tobo, Y., Després, V.R., Garcia, E., Gochis, D.J., Harris, E., Müller- Germann, I., Ruzene, C., Schmer, B., Sinha, B., Day, D.A., Andreae, M.O., Jimenez, J.L., Gallagher, M., Kreidenweis, S.M., Bertram, A.K., Pöschl, U., 2013. High concentrations of biological aerosol particles and ice nuclei during and after rain. Atmos. Chem. Phys. 13, 6151–6164. https://doi.org/10.5194/acp-13-6151-2013.

Irish, V.E., Hanna, S.J., Willis, M.D., China, S., Thomas, J.L., Wentzell, J.J.B., Cirisan, A., Si, M., Leaitch, W.R., Murphy, J.G., Abbatt, J.P.D., Laskin, A., Girard, E., Bertram, A. K., 2019. Ice nucleating particles in the marine boundary layer in the Canadian Arctic during summer 2014. Atmos. Chem. Phys. 19, 1027–1039. https://doi.org/10.5194/acp-19-1027-2019.

Joly, M., Amato, P., Deguillaume, L., Monier, M., Hoose, C., Delort, A.-M., 2014. Quantification of ice nuclei active at near 0 °C temperatures in low-altitude clouds at

the Puy de Dôme atmospheric station. Atmos. Chem. Phys. 14 (8185), 8195. https://doi.org/10.5194/acp-14-8185-2014.
Kanji, Z.A., Ladino, L.A., Wex, H., Boose, Y., Burkert-Kohn, M., Cziczo, D.J., Krämer, M., 2017. Overview of ice nucleating particles. Meteor. Mon. 58 https://doi.org/10.1175/AMSMONOGRAPHS-D-16-0006.1, 1.1–1.33.
Limpert, E., Stahel, W.A., Abbt, M., 2001. Log-normal distributions across the sciences: Keys and clues. BioScience 51, 341–352. https://doi.org/10.1641/0006-3568(2001)051[0341:LNDATS]2.0.CO;2.
Lindemann, J., Constantinidou, H.A., Barchet, W.R., Upper, C.D., 1982. Plants as sources of airborne bacteria, including ice nucleation-active bacteria. Appl. Environ. Microbiol. 44, 1059–1063. https://doi.org/10.1128/aem.44.5.1059-1063.1982.
Mason, B.J., 1996. The rapid glaciation of slightly supercooled cumulus clouds. Q. J. R. Meteorol. Soc. 122, 357–365. https://doi.org/10.1002/qj.49712253003.
Mignani, C., Wieder, J., Sprenger, M.A., Kanji, Z.A., Henneberger, J., Alewell, C., Conen, F., 2021. Towards parameterising atmospheric concentrations of ice-nucleating particles active at moderate supercooling. Atmos. Chem. Phys. 21, 657–664. https://doi.org/10.5194/acp-21-657-2021.
Morrison, H., de Boer, G., Feingold, G., Harrington, J., Shupe, M.D., Sulia, K., 2012. Resilience of persistent Arctic mixed-phase clouds. Nat. Geosci. 5, 11–17. https://doi.org/10.1038/NGEO1332.
Murray, B.J., O'Sullivan, D., Atkinson, J.D., Webb, M.E., 2012. Ice nucleation by particles immersed in supercooled cloud droplets. Chem. Soc. Rev. 41, 6519–6554. https://doi.org/10.1039/c2cs35200a.
Murray, B.J., Carslaw, K.S., Field, P.R., 2021. Opinion: Cloud-phase climate feedback and the importance of ice-nucleating particles. Atmos. Chem. Phys. 21, 665–679. https://doi.org/10.5194/acp-21-665-2021.
Pasquier, J.T., Henneberger, J., Ramelli, F., Lauber, A., David, R.O., Wieder, J., Carlsen, T., Gierens, R., Maturilli, M., Lohmann, U., 2022. Conditions favorable for secondary ice production in Arctic mixed-phase clouds. Atmos. Chem. Phys. 22, 15579–15601. https://doi.org/10.5194/acp-22-15579-2022.
Petters, M.D., Wright, T.P., 2015. Revisiting ice nucleation from precipitation samples. Geophys. Res. Lett. 42, 8758–8766. https://doi.org/10.1002/2015GL065733.
Phillips, V.T.J., Yano, J.-I., Khain, A., 2017. Ice multiplication by breakup in ice-ice collisions. Part I: Theoretical formulation. J. Atmos. Sci. 74, 1705–1719. https://doi.org/10.1175/JAS-D-16-0224.1.
Prenni, A.J., Tobo, Y., Garcia, E., DeMott, P.J., Huffman, J.A., McCluskey, C.S., Kreidenweis, S.M., Prenni, J.E., Pöhlker, C., Pöschl, U., 2013. The impact of rain on ice nuclei populations at a forested site in Colorado. Geophys. Res. Lett. 40, 227–231. https://doi.org/10.1029/2012GL053953.
Rinaldi, M., Hiranuma, N., Santachiara, G., Mazzola, M., Mansour, K., Paglione, M., Rodriguez, C.A., Traversi, R., Becagli, S., Cappelletti, D., Belosi, F., 2021. Ice-nucleating particle concentration measurements from Ny-Ålesund during the Arctic spring–summer in 2018. Atmos. Chem. Phys. 21, 14725–14748. https://doi.org/10.5194/acp-21-14725-2021.
Rodriguez, B., Huang, L., Santos, G., Zhang, W., Vetro, V., et al., 2020. Composition of aerosol in airborne particulate matter and snow at Alert, Canada 2014-2015. Arctic Data Center. https://arcticdata.io/catalog/view/doi%3A10.18739%2FA29W09052 (last access: 29. August 2022).
Sands, D.C., Langhans, V.E., Scharen, A.L., de Smet, G., 1982. The association between bacteria and rain and possible resultant meteorological implications. IDOJARAS - Quarterly Journal of the Hungarian Meteorological Service 86, 148–152. https://www.met.hu/en/ismeret-tar/kiadvanyok/idojaras/index.php?id=1591.
Schaphoff, S., Reyer, C.P.O., Schepaschenko, D., Gerten, D., Shivdenko, A., 2016. Tamm Review: Observed and projected climate change impacts on Russia's forests and its carbon balance. For. Ecol. Manag. 361, 432–444. https://doi.org/10.1016/j.foreco.2015.11.043.
Schneider, J., Höhler, K., Heikkilä, P., Keskinen, J., Bertozzi, B., Bogert, P., Schorr, T., Umo, N.S., Vogel, F., Brasseur, Z., Wu, Y., Hakala, S., Duplissy, J., Moisseev, D., Kulmala, M., Adams, M.P., Murray, B.J., Korhonen, K., Hao, L., Thomson, E.S., Castarède, D., Leisner, T., Petäjä, T., Möhler, O., 2020. Datasets to: the seasonal cycle of ice-nucleating particles linked to the abundance of biogenic aerosol in boreal forests. https://publikationen.bibliothek.kit.edu/1000120666.
Schneider, J., Höhler, K., Heikkilä, P., Keskinen, J., Bertozzi, B., Bogert, P., Schorr, T., Umo, N.S., Vogel, F., Brasseur, Z., Wu, Y., Hakala, S., Duplissy, J., Moisseev, D., Kulmala, M., Adams, M.P., Murray, B.J., Korhonen, K., Hao, L., Thomson, E.S., Castarède, D., Leisner, T., Petäjä, T., Möhler, O., 2021. The seasonal cycle of ice-nucleating particles linked to the abundance of biogenic aerosol in boreal forests. Atmos. Chem. Phys. 21, 3899–3918. https://doi.org/10.5194/acp-21-3899-2021.
Schnell, R.C., Vali, G., 1973. Worldwide souce of leaf derived freezing nuclei. Nature 246, 212–213. https://www.nature.com/articles/246212a0.
Schnell, R., Vali, G., 1976. Biogenic ice nuclei: Part I. Terrestrial and marine sources. J. Atmos. Sci. 33, 1554–1564. https://doi.org/10.1175/15200469(1976)033<1554:BINPIT>2.0.CO;2.
Schrod, J., Thomson, E.S., Weber, D., Kossmann, J., Pöhlker, C., Saturno, J., Ditas, F., Artaxo, P., Clouard, V., Saurel, J.-M., Ebert, M., Curtius, J., Bingemer, H.G., 2020. Long-term deposition and condensation ice-nucleating particle measurements from four stations across the globe. Atmos. Chem. Phys. 20 https://doi.org/10.5194/acp-20-15983-2020, 15 983-16 006.
Seifried, T.M., Bieber, P., Kunert, A.T., Schmale III, D.G., Whitmore, K., Fröhlich-Nowoisky, J., Grothe, H., 2021. Ice nucleation activity of alpine bioaerosol emitted in vicinity of a birch forest. Atmosphere 12, 779. https://doi.org/10.3390/atmos12060779.
Stopelli, E., Conen, F., Morris, C.E., Herrmann, E., Bukowiecki, N., Alewell, C., 2015. Ice nucleation active particles are efficiently removed by precipitating clouds. Sci. Rep. 5, 16433. https://doi.org/10.1038/srep16433.
Sullivan, S.C., Hoose, C., Kiselev, A., Leisner, T., Nenes, A., 2018. Initiation of secondary ice production in clouds. Atmos. Chem. Phys. 18, 1593–1610. https://doi.org/10.5194/acp-18-1593-2018.
Suski, K.J., Hill, T.C.J., Levin, E.J.T., Miller, A., DeMott, P.J., Kreidenweis, S.M., 2018. Agricultural harvesting emissions of ice-nucleating particles. Atmos. Chem. Phys. 18, 13755–13771. https://doi.org/10.5194/acp-18-13755-2018.
Testa, B., Hill, T.C.J., Marsden, N.A., Barry, K.R., Hume, C.C., Bian, Q., Uetake, J., Hare, H., Perkins, R.J., Möhler, O., Kreidenweis, S.M., DeMott, P.J., 2021. Ice nucleating particle connections to regional Argentinian land surface emissions and weather during the Cloud, Aerosol, and Complex Terrain Interactions experiment. J. Geophys. Res: Atmos. 126 https://doi.org/10.1029/2021JD035186 e2021JD035186.
Vali, G., 1971. Quantitative evaluation of experimental results on the heterogeneous freezing nucleation of supercooled liquids. J. Atmos. Sci. 28, 402–409. https://doi.org/10.1175/1520-0469(1971)028<0402:QEOERA>2.0.CO;2.
Vasebi, Y., Mechan Llontop, M.E., Hanlon, R., Schmale III, D.G., Schnell, R., Vinatzer, B. A., 2019. Comprehensive characterization of an aspen (Populus tremuloides) leaf litter sample that maintained ice nucleation activity for 48 years. Biogeosciences 16, 1675–1683. https://doi.org/10.5194/bg-16-1675-2019.
Vergara-Temprado, J., Murray, B.J., Wilson, T.W., O'Sullivan, D., Browse, J., Pringle, K. J., Ardon-Dryer, K., Bertram, A.K., Burrows, S.M., Ceburnis, D., DeMott, P.J., Mason, R.H., O'Dowd, C.D., Rinaldi, M., Carslaw, K.S., 2017. Contribution of feldspar and marine organic aerosols to global ice nucleating particle concentrations. Atmos. Chem. Phys. 17, 3637–3658. https://doi.org/10.5194/acp-17-3637-2017.
Welti, A., Müller, K., Fleming, Z.L., Stratmann, F., 2018a. Concentration and variability of ice nuclei in the subtropical maritime boundary layer. Atmos. Chem. Phys. 18, 5307–5320. https://doi.org/10.5194/acp-18-5307-2018.
Welti, A., Müller, K., Fleming, Z.L., Stratmann, F., 2018b. Time series of ice nuclei concentration at Cape Verde (2009-2013). PANGAEA. https://doi.org/10.1594/PANGAEA.887027.
Wex, H., Huang, L., Zhang, W., Hung, H., Traversi, R., Becagli, S., Sheesley, R., Moffett, J., Barrett, T.E., Bossi, R., Skov, H., Hünerbein, A., Lubitz, J., Löffler, M., Linke, O., Hartmann, M., Herenz, P., Stratmann, F., 2019a. Annual variability of ice-nucleating particle concentrations at different Arctic locations. Atmos. Chem. Phys. 19, 5293–5311. https://doi.org/10.5194/acp-19-5293-2019.
Wex, H., Huang, L., Sheesley, R., Bossi, R., Traversi, R., 2019b. Annual concentrations of ice nucleating particles at Arctic station Ny-Ålesund. PANGAEA. https://doi.org/10.1594/PANGAEA.899696.
Wex, H., Huang, L., Sheesley, R., Bossi, R., Traversi, R., 2019c. Annual concentrations of ice nucleating particles at Arctic station Villum. PANGAEA. https://doi.org/10.1594/PANGAEA.899700.
Wex, H., Huang, L., Sheesley, R., Bossi, R., Traversi, R., 2019d. Annual concentrations of ice nucleating particles at Arctic station Alert. PANGAEA. https://doi.org/10.1594/PANGAEA.899656.
Wex, H., Huang, L., Sheesley, R., Bossi, R., Traversi, R., 2019e. Annual concentrations of ice nucleating particles at Arctic station Barrow/Utqiagvik. PANGAEA. https://doi.org/10.1594/PANGAEA.899698.
Wilson, S.L., Grogan, P., Walker, V.K., 2012. Prospecting for ice association: characterization of freezeethaw selected enrichment cultures from latitudinally distant soils. Can. J. Microbiol. 58, 402e412. https://doi.org/10.1139/W2012-010.
Yang, S., Rojas, M., Coleman, J.J., Vinatzer, B.A., 2022. Identification of candidate ice nucleation activity (INA) genes in Fusarium avenaceum by combining phenotypic characterization with comparative genomics and transcriptomics. Fungi 8, 958. https://doi.org/10.3390/jof8090958.
Zhang, X., Walsh, J.E., Zhang, J., Bhatt, U.S., Ikeda, M., 2004. Climatology and Interannual Variability of Arctic Cyclone activity: 1948–2002. J. Clim. 17, 2300–2317. https://doi.org/10.1175/1520-0442(2004)017<2300:CAIVOA>2.0.CO;2.